Arabian Journal of Chemistry (2023) **16**, 105071

King Saud University

Arabian Journal of Chemistry

www.ksu.edu.sa
www.sciencedirect.com

ORIGINAL ARTICLE

Potential binding of cryptotanshinone with hemoglobin and antimetastatic effects against breast cancer cells through alleviating the expression of MMP-2/-9

Yanling Ma [a,1], Jinjin Sheng [b,1], Fei Yan [a], Wujie Wei [a], Li Li [a], Li Liu [a], Jianhai Sun [a,*]

[a] *Department of Oncology, Hubei No.3 People's Hospital of Jianghan University, Wuhan 430030, China*
[b] *Medical College, Jianghan University, Wuhan 430014, China*

Received 27 April 2023; accepted 10 June 2023
Available online 17 June 2023

KEYWORDS

Cryptotanshinone;
Hemoglobin;
Interaction;
Spectroscopy;
Breast cancer

Abstract As a naturally occurring quinone molecule, cryptotanshinone ($C_{19}H_{20}O_3$) has demonstrated a variety of pharmacological actions through diverse molecular processes. However, the interactions of cryptotanshinone with the major blood proteins and the signaling pathways that contribute to the antimetastatic effect of cryptotanshinone against cancer cells remain largely unknown. The binding of cryptotanshinone to human hemoglobin (Hb) was therefore examined in this study using different spectroscopic techniques such as fluorescence and circular dichroism (CD). To further study the binding interaction at atomic level, molecular docking analysis was also performed. Additionally, cellular assays were performed to assess the anticancer and antimetastatic effects of cryptotanshinone on MCF-7 cells. These assays included cell viability, qPCR, and ELISA assays to measure cell growth as well as mRNA and protein expression of Bax, Bcl-2, matrix metalloproteinase-2 (MMP-2) and MMP-9. According to experimental findings, cryptotanshinone was able to reduce the intrinsic fluorescence [tryptophan (Trp-37)] intensity of hemoglobin (Hb) by a static quenching process, mostly made possible by hydrogen bonding interaction, with no appreciable effects on Hb's secondary structure. Cellular assay showed that cryptotanshinone with a IC_{50} concentration of 17.5 μg/ml can mitigate the breast cancer MCF-7 cell viability through induction of apoptosis (overexpression of Bax/Bcl-2 at both mRNA and protein levels) as well as antimeta-

* Corresponding author at: NO.26, Zhongshan Dadao, Wuhan 430030, Hubei Province, China.
E-mail address: Sunjian.hai@163.com (J. Sun).
[1] Yanling Ma and Jinjin Sheng contributed equally to this study.

Peer review under responsibility of King Saud University. Production and hosting by Elsevier.

Production and hosting by Elsevier

https://doi.org/10.1016/j.arabjc.2023.105071
1878-5352 © 2023 The Authors. Published by Elsevier B.V. on behalf of King Saud University.
This is an open access article under the CC BY-NC-ND license (http://creativecommons.org/licenses/by-nc-nd/4.0/).

static activity (downexpression of MMP-2/-9 at both mRNA and protein levels). In conclusion, we discovered that cryptotanshinone exhibits the potential ability to bind Hb and may be regarded as a promising bioactive anticancer substance, which requires additional *in vitro* research in future studies.

© 2023 The Authors. Published by Elsevier B.V. on behalf of King Saud University. This is an open access article under the CC BY-NC-ND license (http://creativecommons.org/licenses/by-nc-nd/4.0/).

1. Introduction

There is no doubt that breast cancer is among the most common malignancies among women worldwide, making it one of the health organizations' biggest challenges today. (Youn and Han 2020). In the treatment of breast cancer, depending on the patient's condition, various methods such as surgery, chemotherapy, radiation therapy, and hormone therapy are used (Waks and Winer 2019). Because of the side effects and impacts of these treatments on patients' treatment and, on the other hand, the high cost of these methods (Odle 2014), it is imperative that new technologies be applied to find efficient methods with lower costs and side effects against treatment of cancer.

Today, plant-based technology has shown a tremendous interest in the development of a large number of pharmaceuticals, and one of the prospects for the successful treatment of many diseases, notably cancer, is the development of such bioactive materials. Cryptotanshinone ($C_{19}H_{20}O_3$), (R)-1,2,6,7,8,9-hexahydro-1,6,6-trimethyl-phenanthro(1,2-b)furan-10,11-dione, as a naturally occurring quinone substance found mostly in plants of the genus Salvia has long been considered as a potential bioactive compound with different pharmacological activities (Wu, Wu et al. 2020). For instance, it has been demonstrated that blocking Stat3 with cryptotanshinone can cause apoptosis in colorectal cancer cells (Li, Saud et al. 2015) or cryptotanshinone can show anticancer effects against melanoma through ROS-mitochondrial mediated pathway (Ye, Zhu et al. 2016).

It has been also shown that cryptotanshinone mitigates lung cancer metastasis through regulation of microRNA 133a/matrix metalloproteinase (MMP)-14 (Wang, Zhang et al. 2019). In fact, invasion of cancer cells is known as an essential process for metastasis event since these cells must traverse the extracellular matrix to relocate into neighboring tissues. Therefore, cancer metastasis is widely mediated by proteolysis of the extracellular matrix (ECM), which MMPs as the main proteases can play a key role in tumor cell metastasis. MMP-2 and MMP-9 are known as key enzymes contributing to the metastasis signaling pathways. Deactivation of these enzymes could mitigate the induction of tumor metastasis.

Although, the pharmacology activities and molecular mechanisms of bioactive small molecules especially cryptotanshinone have been reported (Wu, Wu et al. 2020), the interaction of this small molecule with blood proteins and signaling pathway involved in the antimetastatic mechanism of cryptotanshinone against MCF-7 cells have not been fully explored.

It has been revealed that protein–small molecule interaction can play a key role in its clinical applications (Yamasaki, Chuang et al. 2013). Also, it has been reported that prediction of drug pharmacokinetic can be done based on *in vitro* studies, deduced by spectroscopic studies (Carvalho, Fernandes et al. 2020). In general, potential binding of therapeutic substances with blood proteins can result in improving their pharmacokinetics (Dennis, Zhang et al. 2002, Mohos, Fliszár-Nyúl et al. 2020). Human hemoglobin (Hb) located in erythrocytes is a main blood protein which has a unique tetramer (two α and two β subunits) structure, mainly composed of α-helical structure. Studies on the interaction of Hb with other small molecules has not been only limited to small molecules (Wang, Zhang et al. 2009, Hu, Wu et al. 2022), but also anionic amphiphiles (De and Girigoswami 2006), ions (Cheng, Lin et al. 2001), and even nanoparticles (Chakraborty, Paul et al. 2018).

Since Hb is considered as a pivotal biofunctional macromolecule for reversible oxygen carrying and storage as well as serving as a carrier protein for small molecule, the potential interaction of cryptotanshinone as a therapeutic bioactive material with Hb as well as alterations of structure and function of Hb after interaction with this ligand could be a focus of this studies. Therefore, the main objective and novelty of this work was to investigate the interaction of cryptotanshinone with Hb through different spectroscopic and molecular docking studies as well as exploring the antimetastatic effects of cryptotanshinone against MCF-7 cells through regulation of MMP-2 and MMP-9 signaling pathway.

2. Materials and methods

2.1. Materials

Lyophilized Hb (Cat No. H7379) and cryptotanshinone [Cat No. C5624, ≥98% (HPLC)] were purchased from Sigma-Aldrich, USA. All other materials were of analytical grades.

2.2. Sample preparation

A 25 μM stock solution of Hb was prepared by dissolving Hb powder in 10 mM phosphate-buffered saline (PBS), pH 7.4. The working concentration of Hb for all spectroscopic studies was fixed at 2.5 μM. Cryptotanshinone was prepared in methanol and further diluted in PBS to make a 200 μM stock solution. Methanol concentration was not above 0.05% (v/v) in final solutions employed in the assays.

2.3. Intrinsic fluorescence study

The fluorescence spectra were read on a Perkin–Elmer LS50B spectrofluorometer with 1-cm quartz cells equipped with a waterbath. The slits for excitation and emission widths were both set at 5 nm. The intrinsic fluorescence intensity of Hb was recorded at 310–450 nm at an excitation wavelength of 295 nm. Hb concentration was fixed at 2.5 μM and added by different concentrations of cryptotanshinone, 2.5 μM, 5 μM, 7.5 μM, 10 μM, 12.5 μM, 15 μM, 17.5 μM, and 20 μM.

2.4. Molecular modeling studies

The molecular docking study was carried out using AutoDock Vina. The three-dimensional (3D) structure of cryptotanshinone was obtained from https://pubchem.ncbi.nlm.nih.gov/compound/Cryptotanshinone with a PubChem CID: 160254. The 3D crystal structure of Hb was downloaded from the Brookhaven Protein Data Bank (https://www.rcsb.org/pdb) with a PDB ID: 2D60. Water molecules were replaced with polar hydrogen and the Gasteiger charges and during the molecular docking study, a maximum of five conformers

were considered for binding study. The structure with the lowest binding free energy was selected for further analysis.

2.5. Far-UV circular dichroism (CD) spectra

The far-UV CD spectra were analyzed by a JASCO CD spectrometer, Model J-815-150S using a 0.1-mm quartz cell. The CD spectra of Hb solutions (2.5 μM) was read alone and in the presence of different concentrations of cryptotanshinone, 2.5 μM, 5 μM, 10 μM, 15 μM, and 20 μM. The spectra were recorded from 260 to 190 nm. Corresponding CD signals derived from cryptotanshinone solution and buffer were also analyzed and subtracted with the same instrumental parameters.

2.6. Cell culture

Human breast adenocarcinoma MCF-7 cell line, American Type Culture Collection (Manassas, VA, USA), were cultured in Delbecco's modified Eagle's medium (DMEM, Gibco/BRL, Gaithersburg, MD. USA) supplemented with 10% fetal bovine serum (Gibco/BRL, Gaithersburg, MD. USA) at 37 °C in a 5% CO_2 atmosphere.

2.7. Cell viability assay

Cell viability assay was done by the 3-(4,5-dimethylthiazol-2-yl)-2,5-diphenyltetrazoliumbromide (MTT) assay. The cells with a density of 1×10^4 cells per well in 96-well plates were plated and after 24 h, the cells were incubated with different concentrations of cryptotanshinone (0, 2.5, 5, and 10, 15, and 20 μM). At 24 h after treatment, the media were gently removed, and the cells were washed thrice with PBS. MTT solution (0.5 mM) was added to each well and incubated for 4 h at 37 °C. Then, the medium was completely removed and 100 μl of dimethyl sulfoxide (DMSO) was added for solubilization of formed crystals. Finally, after shaking the plates for 5 min the optical density was determined at 570 nm using a microplate reader (Bio-Rad, USA).

2.8. Gene expression assay using quantitative real –time PCR

After extracting the total RNA using TRIzol reagent (Invitrogen) following the manufacturer's protocols, RNA was subjected to reverse transcription with Takara cDNA synthesis kit as described in the manufacturer's protocol (Takara Bio Inc., CA). The expression of MMP-2, MMP-9, Bax, and Bcl-2 at mRNA level was assessed by quantitative real-time PCR using the SYBR ExScript RT-PCR kit (TaKaRa, Dalian, China) on an Applied Biosystems 7500 Real-time PCR System (Applied Biosystems, USA). The qPCR program and primers used in this study were based on the previous study (Hobani 2022). β-actin was used as a control reference gene. The data were analyzed using the comparative 2ˆ-ΔΔCt method.

2.9. Protein expression analysis

The levels of protein expression, MMP-2, MMP-9, Bax, and Bcl-2, were analyzed employing colorimetric assays using Bcl-2 (Bender MedSystem, Vienna, Austria), Bax (Assay Designs, USA)), MMP-2 (R&D Systems, Minneapolis, MN, USA), and MMP-9 (RayBiotech, Inc., Norcross, GA, USA) ELISA kit (Neo Biolabs, F Cambridge, MA, USA) according to the manufacturer's instructions.

2.10. Statistical analysis

Data were expressed as mean ± SD (standard deviation) of three experiments. Comparison between groups was done with the one-way analysis of variance (ANOVA). Differences between groups were considered significant at $P < 0.05$.

3. Results and discussion

3.1. Fluorescence quenching study

For proteins, the fluorescence spectroscopy analyses can provide some useful information about the characteristics of binding of bioactive substances to proteins at the atomic level (Hellmann and Schneider 2019). In fact, the calculated parameters including binding mode, binding strength, and thermodynamic parameters derived from fluorescence spectroscopic studies can be used to evaluate the binding characteristics of ligand/protein (Khan, Cho et al. 2023). According to the X-ray crystallographic data (Safo and Abraham 2003), Hb with a predominant α-helix structure contains a relatively rigid conformer, two α-chains (141 residues) and two β-chains (146 amino acid residues), and 6 tryptophan (Trp) residues, two α Trp 14, two β Trp 15, and two β Trp 37. Trp 37 exists at the αβ–αβ interface, provides the most dominant fluorophores, and shows a potential ligand binding affinity (Safo and Abraham 2003, Kaur, Singh et al. 2023). Therefore, fluorescence spectroscopy study is a sensitive technique to examine the microenvironmental changes around Trp 37 amino acid residues. Fig. 1 (A, B, C) exhibits Hb fluorescence intensity after interaction with different concentrations of cryptotanshinone. As the data display, the fluorescence intensity of Hb reduced continuously with the elevating concentration of cryptotanshinone, which reveals that this small molecule substrate can potentially interact with Hb. Also, the observation of a slight red shift, especially at 303 K (Fig. 1B) and 308 K (Fig. 1C) could demonstrate that probable subtle conformational changes of Hb triggered by the interaction of cryptotanshinone were associated with the displacement of Trp residues to a hydrophilic microenvironment. In general, the result indicates that binding of cryptotanshinone to Hb has no (at 298 K) or little (at 303 K and 308 K) effect on the microenvironment around Trp 37 residue.

3.1.1. Fluorescence quenching mechanisms

The different quenching mechanisms of proteins are usually categorized as either dynamic, static, or mixed (Zhang, Cho et al. 2022). Dynamic quenching is associated with a system of collisional interactions between the protein and substrate and the resultant quenching during the excited state lifetime (Sett, Paul et al. 2022). Static quenching derives from the ground-state complex formation between the protein and the substrate (Kenoth and Kamlekar 2022). For determination of fluorescence quenching, the reduction in fluorescence inten-

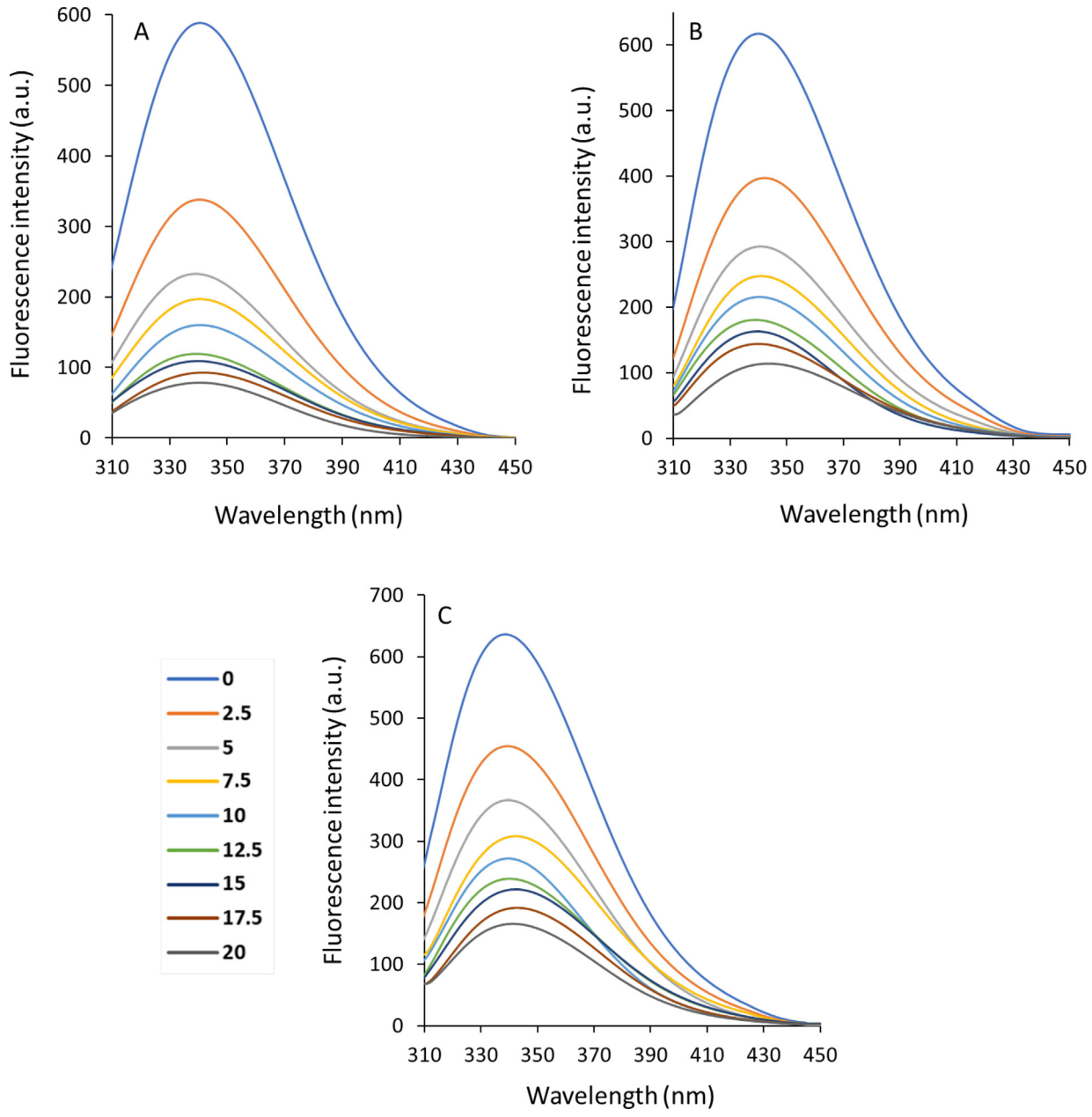

Fig. 1 Emission spectra of Hb with a concentration of 2.5 μM in the presence of different concentrations of cryptotanshinone (2.5–20 μM) at 298 K (A), 303 K (B) and 308 K (C).

sity is typically assessed by the Stern–Volmer equation (Wang, Zhang et al. 2008):

$$F_0/F = 1 + k_q\tau_0[Q] = 1 + K_{SV}[Q] \quad (1)$$

where F_0 and F are the steady-state emission of free and bound proteins, respectively. kq and τ_0 are the bimolecular quenching constant and the lifetime of the emission without substrate (5.0 ns), respectively (Gryczynski, Beretta et al. 1997). [Q] and K_{SV} are the concentration of substrate and Stern–Volmer quenching constant, respectively. Fig. 2 depicts the Stern–Volmer plots of Hb fluorescence quenching by cryptotanshinone. In the present study, a linear Stern–Volmer plot was observed for cryptotanshinone (Fig. 2), meaning that the quenching mechanism should be either single static or dynamic, and no mixed quenching mechanism could contribute in the formation of Hb-cryptotanshinone complex. For the presence of dynamic quenching, higher temperatures usually cause faster diffusion and subsequent larger value of collisional quenching (Mandal and Ganguly 2009). Therefore, the K_{SV} enhances with increasing temperature for dynamic quenching mechanism, however the reverse influence could be expected for static quenching mechanism. Also, the maximum value of collision quenching constant of a protein, k_q, has been reported to be 2×10^{10} M^{-1} s^{-1} (Mandal and Ganguly 2009).

The values of K_{SV} calculated from the slope of the Stern-Volmer plot are summarized in Table 1. The data showed that the values of K_{SV} for cryptotanshinone are 3.17×10^5 M^{-1},

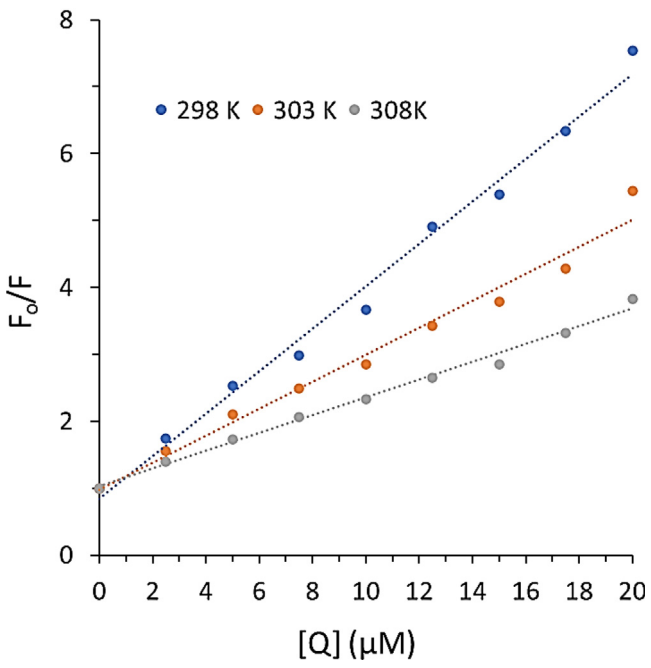

Fig. 2 Stern-Volmer plots of Hb after interaction with cryptotanshinone at three temperatures.

2.01×10^5 M^{-1}, and 1.33×10^5 M^{-1} at 298 K, 303 K, and 308 K. This data showed that the K_{SV} values are not directly correlated with temperature. Also, the values of k_q (6.34–2.66 $\times 10^{13}$ $M^{-1}s^{-1}$) were much > 2×10^{10} M^{-1} s^{-1} (Table 1). All these data indicated that the quenching mechanism of Hb by cryptotanshinone is based on a static quenching type.

It has been reported that Hb contains three Trp residues per αβ dimmer and there are often remarkable variations in the accessibility of these residues to the solvent and ligand, revealing local protein conformation that cause deviations from linearity in the Stern–Volmer plot (Yang, Cheng et al. 2018). However, Fig. 2 showed a good linearity of Stern-Volmer plot, suggesting a similar fluorophore accessibility of Trp residues, mainly Trp 37, to the cryptotanshinone. Therefore, we can conclude that the quenching mechanism of Hb by cryptotanshinone is based on a static quenching at all studied concentrations (2.5–20 μM) and the "sphere of action" quenching mechanism does not play a key role in our studied system (Yang, Cheng et al. 2018).

3.1.2. Binding parameters

In the present research, the binding parameters were evaluated by analyzing the cryptotanshinone triggered fluorescence quenching data of Hb. The binding constant (K_b) and the number of binding sites (n) were estimated according to Eq. (2) (Hamishehkar, Hosseini et al. 2016):

$$\log F_0 - F/F = \log K_b + n \log [Q] \quad (2)$$

where all parameters are similar to Eq. (1). Fig. 3 shows the plots of log (F_0 − F)/F versus log [Q] for the studied cryptotanshinone–Hb systems at different temperatures of 298, 303 K, and 308 K.

The calculated values of K_b and the n are presented in Table 2. For the cryptotanshinone –Hb system, the values of K_b decreased with increasing temperature, indicating the binding process occurs through an exothermic process (Shen, Liou et al. 2007). In fact, the values of K_b of Hb with cryptotanshinone at three different temperatures were in the following order as: 298 K > 303 K > 308 K. It is clear that cryptotanshinone interacts with Hb with larger K_b at 298 K, revealing cryptotanshinone binds Hb in a more firmly manner at 298 K than the other two higher temperatures, 303 K and 308 K. Furthermore, it was shown that the value of K_b was in magnitude of 10^5 at 298 K, suggesting a strong binding affinity between cryptotanshinone and Hb, which reduce to 10^4 at higher temperature. In fact, at 308 K close to physiological temperature, the K_b value is in a magnitude of 10^4, revealing a moderate binding affinity (Kou, Li et al. 2023) between Hb and cryptotanshinone. Therefore, we can claim that cryptotanshinone can interact with Hb with a moderate binding affinity at physiological temperature, which can be considered as a potential interaction for therapeutic small molecules, *in vivo*.

Moreover, the values of n were calculated to be approximately equal to 1, suggesting that there was a single class of binding sites on Hb for cryptotanshinone. In Hb, the Trp 37 is exposed to a polar environment, so from the calculated value of n, it may be deduced that cryptotanshinone most likely interacts with the Trp 37 and leads to a remarkable quenching in its intrinsic fluorescence intensity.

3.1.3. Binding mode

Generally discussing, the forces between organic biomolecules and biomacromolecules are categorized into hydrogen bonding, van der Waals, electrostatic, and hydrophobic (Odle, 2014). The signs as well as the magnitudes of thermodynamic parameters for protein-small molecule interactions can reveal the predominant forces responsible for the formation of the corresponding complex. If we suppose that the enthalpy changes (ΔH) are almost unchanged over the temperature range analyzed, then the associated value can be estimated from the well-known van't Hoff Eq. (3) (Chowdhury, Bhuiya et al. 2020):

$$\ln K_b = -\Delta H/RT + \Delta S/R \quad (3)$$

K_b is the binding constant at temperature T and R is defined as the gas constant. The value of ΔH and entropy changes (ΔS) can be obtained from linear van't Hoff plot. The value of Gibbs free energy changes (ΔG) was then calculated from the following Eq. (4) (Salam, Arif et al. 2023):

Table 1 The values of quenching parameters for interaction of Hb and cryptotanshinone at different temperatures.

T (K)	K_{SV} $(M^{-1})_{\times 10}$	k_q $(M^{-1}\ s^{-1})_{\times 10^{13}}$	R^2	Equation
298	3.17	6.34	0.98	y = 0.3173x + 0.8396
303	2.01	4.02	0.97	y = 0.2015x + 0.9786
308	1.33	2.66	0.99	y = 0.133x + 1.0244

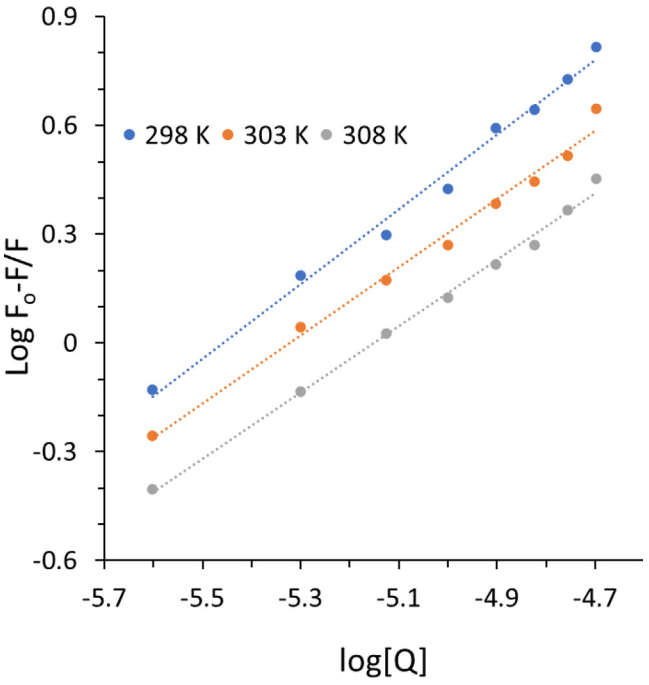

Fig. 3 Modified Stern-Volmer plots of Hb after interaction with cryptotanshinone at three temperatures.

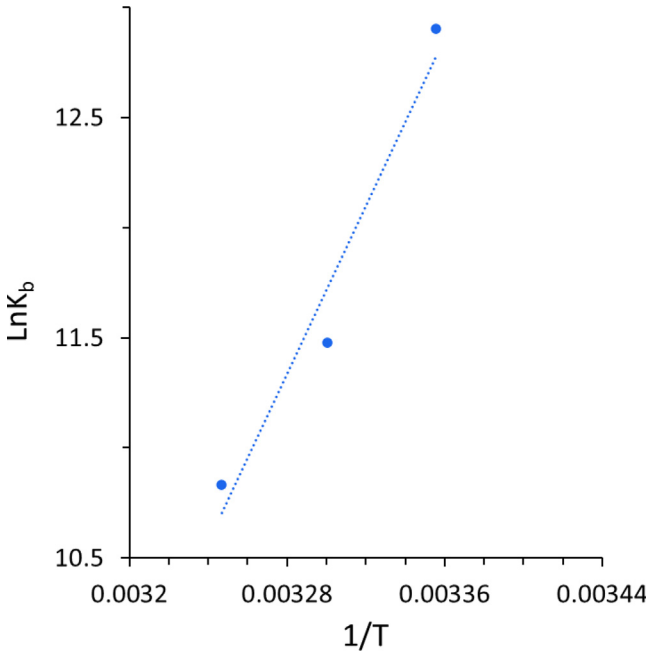

Fig. 4 van't Hoff plot for the binding reaction between Hb and cryptotanshinone.

$$\Delta G = \Delta H - T\Delta S \quad (4)$$

From the linear correlation between lnK_b and the reciprocal T (Fig. 4), the values of ΔH and ΔS can be obtained and presented in Table 3.

As listed in Table 3, values of ΔH and ΔS for the binding reaction between Hb and cryptotanshinone were found to be -158.00 kJ mol^{-1} and -424.15 J mol^{-1} K^{-1}, which suggested that the binding process for the interaction between Hb and cryptotanshinone was based on an exothermic reaction. The negative sign for ΔG revealed the spontaneity of the interaction of cryptotanshinone with Hb. Ross and Subramanian (Ross and Subramanian 1981) have evaluated the sign and magnitude of the thermodynamic parameters linked with different individual types of interaction between small molecules and proteins. Based on the water structure viewpoint, a negative ΔS value is mostly considered as a typical fact for the formation of hydrogen bonds, because the water molecules surrounded small molecule and receptor are rearranged in an ordered configuration as a result of hydrogen bonding (Zeinabad, Kachooei et al. 2016). Further, the negative ΔH value calculated could not be typically assigned to the contribution of electrostatic forces since for such interactions the value of ΔH should be very small. The negative ΔH value is mainly associated with the contribution of hydrogen bonding in the interaction of this ligand with macromolecules (Ross and Subramanian 1981). Therefore, from the negative values of ΔH and ΔS calculated in the present study, we can claim that the main acting forces in the formation of cryptotanshinone-Hb complex are mostly hydrogen bonding and van der Waals forces.

Table 3 The values of thermodynamic parameters for the binding reaction between Hb and cryptotanshinone at different temperatures.

T (K)	$\Delta H°$ (kJ/mol)	$\Delta S°$ (J/mol. K)	$\Delta G°$ (kJ/mol)
298	−158.00	−424.15	−31.61
303	−158.00	−424.15	−29.49
308	−158.00	−424.15	−27.36

3.2. Molecular modeling study

Molecular modeling of the small molecules with receptors provides some helpful data with reference to the favorable binding pockets and can be exploited to confirm the experimental results at atomic level (Rudra, Dasmandal et al. 2018, Salam, Arif et al. 2023). The most probable binding mode between cryptotanshinone (Fig. 5A) and Hb to form a cryptotanshinone-Hb complex is shown in Fig. 5B. The docking results revealed a strong interaction between cryptotanshi-

Table 2 The values of binding parameters for interaction of Hb and cryptotanshinone at different temperatures.

T (K)	$logK_b$ M^{-1}	n	R^2	Equation
298	5.61	1.02	0.99	y = 1.0285x + 5.6145
303	4.99	0.93	0.98	y = 0.9383x + 4.9943
308	4.71	0.91	0.99	y = 0.9154x + 4.7157

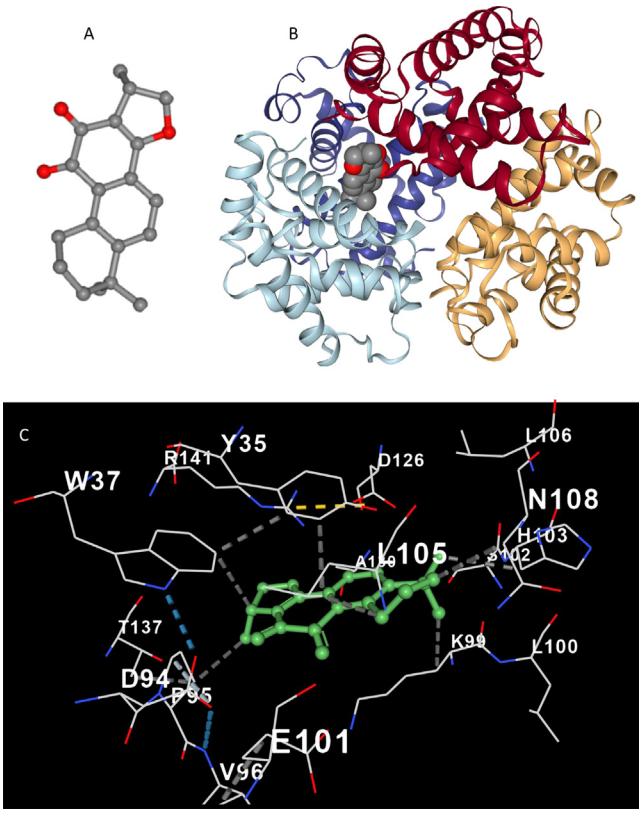

Fig. 5 3D structure of cryptotanshinone(A), docking result of cryptotanshinone-Hb complex (B), amino acid residues in the binding pocket of cryptotanshinone-Hb complex (C).

none and Hb with a binding score of −8.3 kcal/mol, which is in good agreement with thermodynamic parameters deduced by intrinsic fluorescence spectroscopic study. From Fig. 5B, we can find that most preferential binding sites of the cryptotanshinone on Hb are close to αβ–αβ interface. The interaction between cryptotanshinone and Hb at the binding site is mediated by Pro 95, Trp 37, Tyr 35, Lys 99, Asn 108, Leu 105, Leu 66, Val 62, Val 132, Leu136, Phe 43, and Val 93 amino acid residues (Fig. 5C), contributing in the formation of hydrophilic and hydrophobic forces.

Molecular docking analysis also supported the fluorescence spectroscopy data, as it shows that Trp 37 and Tyr 35 are located in the binding site of Hb after interaction with cryptotanshinone (Fig. 5C). It was found that Trp 37 directly interacts with cryptotanshinone, while Try 35 in the binding site is not involved in the direct establishment of hydrophilic or hydrophobic forces between cryptotanshinone and Hb. This data also is in good agreement with intrinsic fluorescence spectroscopy results, indicating that the fluorescence quenching of Hb induced by cryptotanshinone is based on a direct interaction between Trp 37 residue and cryptotanshinone.

3.3. Circular dichroism study

To gain further information in cryptotanshinone –Hb interaction mechanism and conformational alteration of protein, CD study (Panchal, Sehrawat et al. 2023) was done on Hb and cryptotanshinone–Hb complex. Fig. 6. depicts the CD spectra of Hb either in free state or in combination with various concentrations of cryptotanshinone at pH 7.40 and 298 K. The CD spectrum of Hb is characterized by two main negative ellipticity changes centered around 208 and 222 nm, revealing the dominance of an α-helical structure (Salam, Arif et al. 2023). It was detected from Fig. 6 that there was a slight

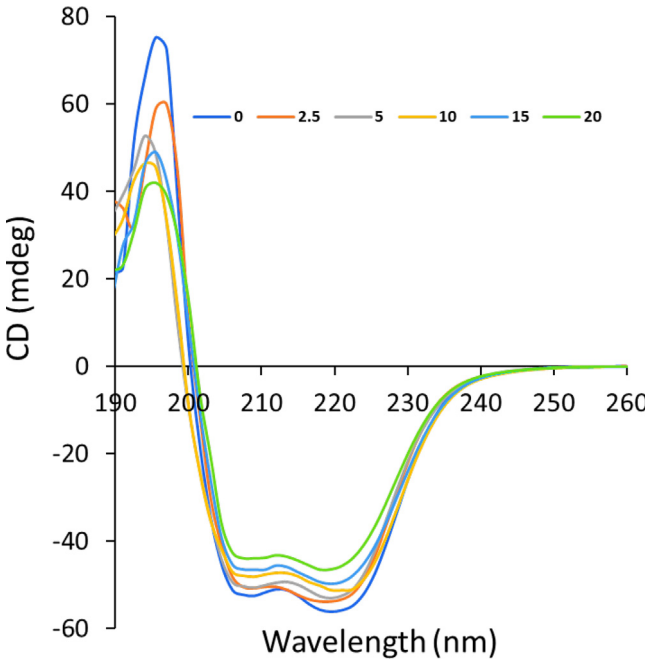

Fig. 6 Far-UV CD study of Hb with a concentration of 2.5 μM in the presence of different concentrations of cryptotanshinone (2.5–20 μM) at 298 K.

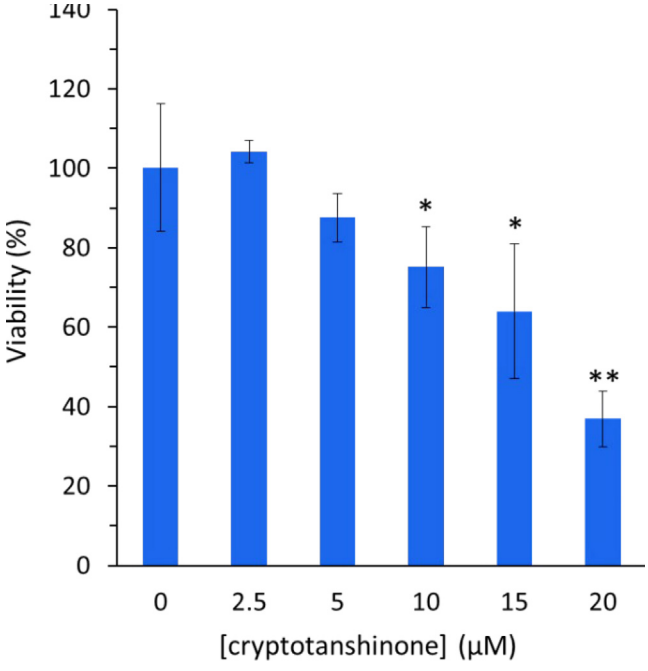

Fig. 7 MTT assay for determination of the cytotoxic effect of cryptotanshinone on the proliferation of MCF-7 cells at various concentrations for 24 h. All the experiments were carried in triplicate, and data are reported as mean ± SD values. *P < 0.05, **P < 0.01, relative to control.

decrease in ellipticity changes of both of these minima without any apparent shift in the positions of these peaks, meaning the negligible decrease in the α-helical content of Hb after interaction with cryptotanshinone. It is clear that interaction of cryptotanshinone with Hb led to slight secondary structural changes of Hb, leading to a slight loss of α-helical biostability (Panchal, Sehrawat et al. 2023).

The calculating results done by CDNN software (http//bioinformatik.biochemtech.uni-halle.de/cdnn) revealed a reduction of α-helical structures from 60.89% to 60.48%, 59.37%, 57.25%, 55.55%, and 54.21% at different 0 μM, 2.5 μM, 5 μM, 10 μM, and 20 μM of cryptotanshinone, respectively. Therefore, this observation shows that although slight changes was observed in the secondary structure of Hb as expected for the interaction of small molecules with proteins but the total secondary structure of Hb was mostly unchanged and its integrity was almost preserved even after interaction with cryptotanshinone at highest studied concentration (20 μM). As a result, upon interaction of 20 μM with biomacromolecules like Hb, no significant changes in the secondary structure of the proteins can be expected. All the above data indicated that cryptotanshinone could be used as potential therapeutic agents in biomedical applications *in vitro* and *in vivo*.

3.4. Cell viability assay

MTT assay was utilized to assess the cytotoxicity of cryptotanshinone on breast cancer MCF-7 cell line. Fig. 7 shows the cytotoxicity of cryptotanshinone on the tested cell line at 24 h. Cryptotanshinone showed a concentration dependent cytotoxicity against the tested cell line. Therefore, following incubation of the MCF-7 cells for 24 h with cryptotanshinone, the growth inhibitory properties of cryptotanshinone were explored. It was seen that the values of cell viability were 104.24%, 87.62%, 75.15%, 64.01%, and 36.95% after interaction with 2.0 μM, 5 μM, 10 μM, 15 μM, and 20 μM cryptotanshinone, respectively (Fig. 7). The cryptotanshinone IC_{50} value on inhibiting the proliferation of MCF-7 was around 17.5 μg/ml in a 24-h incubation period which was comparable with the previous study reported on the effect of cryptotanshinone on breast cancer MCF-7 cells (Shi, Li et al. 2022).

3.5. Effect of cryptotanshinone on apoptosis induction in MCF-7 cells

Apoptosis-mediated cell death can be modulated by different anticancer drugs. In fact, anticancer compounds can switch on apoptosis signaling pathways through different mechanisms in cancer cells. To assess the mechanism of cytotoxicity stimulated by cryptotanshinone, apoptosis (programmed cell death) was examined and the data are expressed in Fig. 8. The levels of Bcl-2 and Bax in the mitochondria can mediate the induction of apoptosis induced by bioactive materials through an intrinsic mechanism (Sanaei and Kavoosi 2021). For the potential modulation of mitochondria-mediated apoptosis, a balance between the pro-apoptosis performance of Bax and

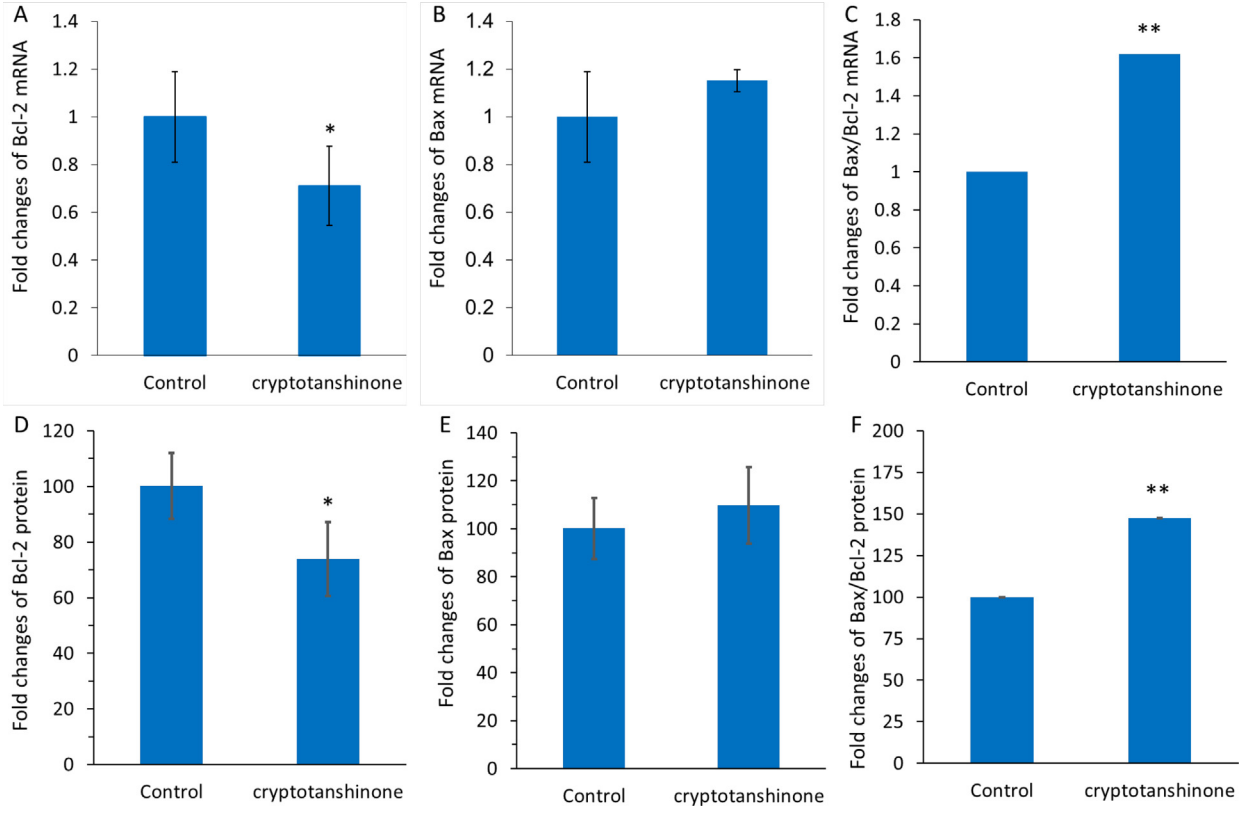

Fig. 8 Qpcr assay for assessing the expression of bcl-2 mrna (A), bax mrna (B), and bax/bcl-2 mrna ratio (C) after incubation of mcf-7 cells with cryptotanshinone (17.5 μM) at 24 h. ELISA assay for determination of the expression of Bcl-2 protein (D), Bax protein (E), and Bax/Bcl-2 protein ratio (F) after incubation of MCF-7 cells with cryptotanshinone (17.5 μM) at 24 h. All the experiments were carried in triplicate, and data are reported as mean ± SD values. *P < 0.05, **P < 0.01, ***P < 0.001, relative to control.

anti-apoptosis function of Bcl2 should have existed (Singh, Letai et al. 2019). The relocation of Bax into mitochondria triggers mitochondrial dysfunction, which could result in the potentiation of small molecules-stimulated apoptosis (Hafezi and Rahmani 2021). Apoptosis triggered by cryptotanshinone can be assosiated with the enhanced pro-apoptotic mRNA/protein levels and/or reduced antiapoptotic mRNA/protein expression, meaning that the Bax/Bcl-2 ratio may be an important apoptotic signal induced by this small molecule. In this paper, it was found that cryptotanshinone significantly reduced the expression of Bcl-2 at mRNA level (Fig. 8A), while the Bax mRNA level was not significantly changed (Fig. 8B). In general, it was revealed that the Bax/Bcl-2 ratio at mRNA level was significantly increased in cryptotanshinone-treated MCF-7 cells relative to control cells (Fig. 8C), revealing that cryptotanshinone can induce apoptosis in MCF-7 cells. To further support this experiment, the expression of Bax and Bcl-2 at protein level was also revealed by ELISA assay. In this study, cryptotanshinone induced a similar pattern of downexpression of Bcl-2 (Fig. 8D), overexpression of Bax (Fig. 8E) as well as overexpression of Bax/Bcl-2 (Fig. 8F) at protein level to those observed in mRNA level, suggesting that this bioactive compound is able to stimulate apoptosis by acting on an intrinsic pathway in MCF-7 cells.

Similar results have been reported earlier. For example, cryptotanshinone inhibited lung tumorigenesis through induction of apoptosis mediated by overexpression of p53 and Bax and downregulation of Bcl-2 (Chen, Wang et al. 2014). Ke et al. also reported that cryptotanshinone triggers cell cycle arrest and apoptosis in cholangiocarcinoma cells by increased Bax/Bcl-2 ratio (Ke, Wang et al. 2017). Furthermore, a few other abietane diterpenoid such as parvifloron D (Burmistrova, Perdomo et al. 2015) or derived from *Salvia chloroleuca* (Shakeri, Delavari et al. 2019) as well as *Salvia sahendica* (Kafil, Eskandani et al. 2015) have demonstrated a similar type of apoptosis-mediated cell death against different cancers. Accordingly, in the current study, cryptotanshinone appears to induce anticancer effect against MCF-7 cells through regulating the Bax/Bcl-2 ratio, and the augmented Bax/Bcl-2 expression at both mRNA and protein levels in MCF-7 cells can result in the apoptosis.

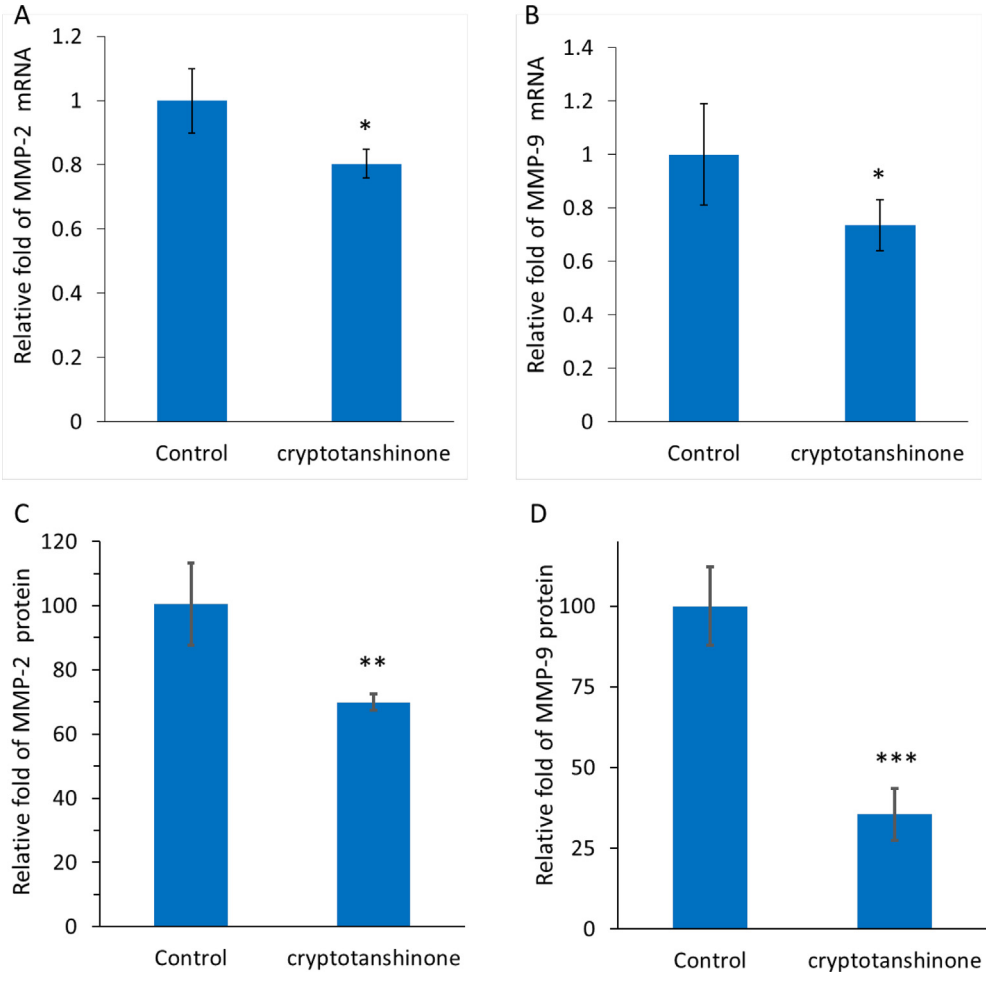

Fig. 9 qPCR assay for determining the expression of MMP-2 mRNA (a) and MMP-9 mRNA (b) in MCF-7 cells incubated with cryptotanshinone (17.5 μM) at 24 h. ELISA assay for determination of the expression of MMP-2 protein (C) and MMP-9 protein (D) in MCF-7 cells incubated with cryptotanshinone (17.5 μM) at 24 h. All the experiments were carried in triplicate, and data are reported as mean ± SD values. *P < 0.05, **P < 0.01, ***P < 0.001, relative to control.

3.6. Effects of cryptotanshinone on invasion mRNA and protein expression in MCF-7 cells

Real-time PCR and ELISA assays were also carried out to assess the mRNA and protein expression levels of invasion-associated main mediators in MCF-7 cells, MMP-2 and MMP-9, after treatment with IC_{50} concentration of cryptotanshinone at 24 h. As shown in Figure 9A, B, a significant downxpression in the MMP-2 and MMP-9 mRNA levels in 17.5 μM cryptotanshinone-treated MCF-7 cells in comparison with control cells was observed. Also, ELISA-assisted protein expression assays showed that at 24 h, there was a significant decrease in the MMP-2 (Fig. 9C) and MMP-9 (Fig. 9D) protein levels in MCF-7 cells treated with cryptotanshinone relative to control cells. Therefore, it was deduced that IC_{50} concentration of cryptotanshinone at 24 h mitigated the MMP-2 and-9 protein expression (Fig. 9C, D) in the same pattern as it was detected at the mRNA level (Fig. 9A, B).

Metastasis in cancer cells is multifactorial and multistep, and it mainly includes invasion and migration of cells (de Visser and Joyce 2023, Yuan, Li et al. 2023). Anti-metastatic drugs can regulate these mechanisms, resulting in less metastatic cancer/tumor cells. (Fares, Fares et al. 2020). MMPs are known as essential extracellular matrix enzymes catalyzing the degradation of proteins (Gonzalez-Avila, Sommer et al. 2019, Paolillo and Schinelli 2019). These enzymes can contribute apparently to cancer cell metastasis by degrading the extracellular proteins (Mehner, Hockla et al. 2014). MMPs are significantly overexpressed in breast cancer cells which can mediate their metastasis. As a result, bioactive small molecules-mediated MMP inhibition can play a key role in mitigation of metastasis in breast cancer cells (Radisky and Radisky 2010, Javadian, Gharibi et al. 2019). Inhibition of the expression of molecular mediators including MMP-2 and MMP-9 as main enzymes involved in the metastasis progression, can result in the control of cancer metastasis (Conlon and Murray 2019). Our experimental data suggested that cryptotanshinone in MCF-7 cells could downregulate the MMP-2 and MMP-9 at both mRNA and protein levels. Similar to our result, Wang et al., reported that cryptotanshinone is able to inhibit lung cancer metastasis through regulation of microRNA 133a/MMP-14 (Wang, Zhang et al. 2019). Also, Zhang et al., indicated that cryptotanshinone triggers apoptosis and regulates metastasis in human hepatocellular carcinoma cells through control of MMPs-mediated signaling pathway (Zhang, Wang et al. 2020).

4. Conclusions

This report expresses spectroscopic and molecular docking investigations on the interaction of cryptotanshinone with Hb using fluorescence emission and CD spectra. It was realized that the fluorescence of Hb was quenched for interaction with cryptotanshinone based on a type of static fluorescence quenching. All thermodynamic parameters were negative, revealing that and the main binding force between cryptotanshinone and Hb was probably hydrogen bonding interaction. The binding site was close to Trp-37 and Tyr 35 in Hb as evidenced by molecular docking study. It was also found that cryptotanshinone did not induce a significant effect on the secondary structure of Hb. Cellular assays showed that cryptotanshinone induced anticancer effects in breast cancer MCF-7 cell line through overexpression of -Bax/Bcl-2 ratio and down regulation of MMP-2 and MMP-9 at both transcriptional and translational levels. In conclusion, the data presented here indicated that cryptotanshinone may interact with Hb and can be considered a significant naturally occurring anticancer substance for the development of therapeutic platforms, however more *in vivo* and pre-clinical research is required.

Funding

This study was supported by Key Scientific Research Project of Wuhan Municipal Health and Wellness Committee, No. WX20B21.

Declaration of Competing Interest

The authors declare that they have no known competing financial interests or personal relationships that could have appeared to influence the work reported in this paper.

References

Burmistrova, O., Perdomo, J., Simões, M.F., Rijo, P., Quintana, J., Estevez, F., 2015. The abietane diterpenoid parvifloron D from Plectranthus ecklonii is a potent apoptotic inducer in human leukemia cells. Phytomedicine 22 (11), 1009–1016.

Carvalho, A.M., Fernandes, E., Gonçalves, H., Giner-Casares, J.J., Bernstorff, S., Nieder, J.B., Oliveira, M.E.C.D.R., Lúcio, M., 2020. Prediction of paclitaxel pharmacokinetic based on in vitro studies: Interaction with membrane models and human serum albumin. Int. J. Pharm. 580, 119222.

Chakraborty, M., Paul, S., Mitra, I., Bardhan, M., Bose, M., Saha, A., Ganguly, T., 2018. To reveal the nature of interactions of human hemoglobin with gold nanoparticles having two different morphologies (sphere and star-shaped) by using various spectroscopic techniques. J. Photochem. Photobiol. B Biol. 178, 355–366.

Chen, L., Wang, H.-J., Xie, W., Yao, Y., Zhang, Y.-S., Wang, H., 2014. Cryptotanshinone inhibits lung tumorigenesis and induces apoptosis in cancer cells in vitro and in vivo. Mol. Med. Rep. 9 (6), 2447–2452.

Cheng, Y., Lin, H., Xue, D., Li, R., Wang, K., 2001. Lanthanide ions induce hydrolysis of hemoglobin-bound 2, 3-diphosphoglycerate (2, 3-DPG), conformational changes of globin and bidirectional changes of 2, 3-DPG-hemoglobin's oxygen affinity. Biochimica et Biophysica Acta (BBA)-Molecular Basis of Disease 1535 (2), 200–216.

Chowdhury, S., Bhuiya, S., Haque, L., Das, S., 2020. In-depth investigation of the binding of flavonoid taxifolin with bovine hemoglobin at physiological pH: Spectroscopic and molecular docking studies. Spectrochim. Acta A Mol. Biomol. Spectrosc. 225, 117513.

Conlon, G.A., Murray, G.I., 2019. Recent advances in understanding the roles of matrix metalloproteinases in tumour invasion and metastasis. J. Pathol. 247 (5), 629–640.

De, S., Girigoswami, A., 2006. A fluorimetric and circular dichroism study of hemoglobin—Effect of pH and anionic amphiphiles. J. Colloid Interface Sci. 296 (1), 324–331.

de Visser, K.E., Joyce, J.A., 2023. The evolving tumor microenvironment: From cancer initiation to metastatic outgrowth. Cancer Cell 41 (3), 374–403.

Dennis, M.S., Zhang, M., Meng, Y.G., Kadkhodayan, M., Kirchhofer, D., Combs, D., Damico, L.A., 2002. Albumin binding as a general strategy for improving the pharmacokinetics of proteins. J. Biol. Chem. 277 (38), 35035–35043.

Fares, J., Fares, M.Y., Khachfe, H.H., Salhab, H.A., Fares, Y., 2020. Molecular principles of metastasis: a hallmark of cancer revisited. Signal Transduct. Target. Ther. 5 (1), 28.

Gonzalez-Avila, G., Sommer, B., Mendoza-Posada, D.A., Ramos, C., Garcia-Hernandez, A.A., Falfan-Valencia, R., 2019. Matrix metalloproteinases participation in the metastatic process and their diagnostic and therapeutic applications in cancer. Crit. Rev. Oncol. Hematol. 137, 57–83.

Gryczynski, Z., Beretta, S., Lubkowski, J., Razynska, A., Gryczynski, I., Bucci, E., 1997. Time-resolved fluorescence of hemoglobin species. Biophys. Chem. 64 (1–3), 81–91.

Hafezi, S., Rahmani, M., 2021. Targeting BCL-2 in cancer: advances, challenges, and perspectives. Cancers 13 (6), 1292.

Hamishehkar, H., Hosseini, S., Naseri, A., Safarnejad, A., Rasoulzadeh, F., 2016. Interactions of cephalexin with bovine serum albumin: displacement reaction and molecular docking. Bioimpacts 6 (3), 125.

Hellmann, N., Schneider, D., 2019. Hands on: using tryptophan fluorescence spectroscopy to study protein structure. Protein Supersecondary Structures: Methods and Protocols, 379–401.

Hobani, Y.H., 2022. Cytotoxicity of Mahanimbine from Curry Leaves in Human Breast Cancer Cells (MCF-7) via Mitochondrial Apoptosis and Anti-Angiogenesis. Molecules 27 (3), 971.

Hu, X., Wu, D., Tang, L., Zhang, J., Zeng, Z., Geng, F., Li, H., 2022. Binding mechanism and antioxidant activity of piperine to hemoglobin. Food Chem. 394, 133558.

Javadian, M., Gharibi, T., Shekari, N., Abdollahpour-Alitappeh, M., Mohammadi, A., Hossieni, A., Mohammadi, H., Kazemi, T., 2019. The role of microRNAs regulating the expression of matrix metalloproteinases (MMPs) in breast cancer development, progression, and metastasis. J. Cell. Physiol. 234 (5), 5399–5412.

Kafil, V., Eskandani, M., Omidi, Y., Nazemiyeh, H., Barar, J., 2015. Abietane diterpenoid of Salvia sahendica Boiss and Buhse potently inhibits MCF-7 breast carcinoma cells by suppression of the PI3K/AKT pathway. RSC Adv. 5 (23), 18041–18050.

Kaur, L., Singh, A., Datta, A., Ojha, H., 2023. Multispectroscopic studies of binding interaction of phosmet with bovine hemoglobin. Spectrochim. Acta A Mol. Biomol. Spectrosc. 122630

Ke, F., Wang, Z., Song, X., Ma, Q., Hu, Y., Jiang, L., Zhang, Y., Liu, Y., Zhang, Y., Gong, W., 2017. Cryptotanshinone induces cell cycle arrest and apoptosis through the JAK2/STAT3 and PI3K/Akt/NFκB pathways in cholangiocarcinoma cells. Drug Des. Devel. Ther., 1753–1766

Kenoth, R. and Kamlekar, R. K. 2022. Steady-State Fluorescence Spectroscopy as a Tool to Monitor Protein/Ligand Interactions. Optical Spectroscopic and Microscopic Techniques: Analysis of Biological Molecules, Springer: 35-54.

Khan, S., Cho, W.C., Hussain, A., Azimi, S., Babadaei, M.M.N., Bloukh, S.H., Edis, Z., Saeed, M., Ten Hagen, T.L.M., Ahmadi, H., 2023. The interaction mechanism of plasma iron transport protein transferrin with nanoparticles. Int. J. Biol. Macromol. 124441.

Kou, S.-B., Li, L., Zhang, R.-J., Shi, J.-H., Jiang, S.-L., 2023. Elucidation of the interaction mechanism of olmutinib with human α-1 acid glycoprotein: insights from spectroscopic and molecular modeling studies. J. Biomol. Struct. Dyn. 41 (2), 525–537.

Li, W., Saud, S.M., Young, M.R., Colburn, N.H., Hua, B., 2015. Cryptotanshinone, a Stat3 inhibitor, suppresses colorectal cancer proliferation and growth in vitro. Mol. Cell. Biochem. 406, 63–73.

Mandal, P., Ganguly, T., 2009. Fluorescence spectroscopic characterization of the interaction of human adult hemoglobin and two isatins, 1-methylisatin and 1-phenylisatin: a comparative study. J. Phys. Chem. B 113 (45), 14904–14913.

Mehner, C., Hockla, A., Miller, E., Ran, S., Radisky, D.C., Radisky, E.S., 2014. Tumor cell-produced matrix metalloproteinase 9 (MMP-9) drives malignant progression and metastasis of basal-like triple negative breast cancer. Oncotarget 5 (9), 2736.

Mohos, V., Fliszár-Nyúl, E., Lemli, B., Zsidó, B.Z., Hetényi, C., Mladěnka, P., Horký, P., Pour, M., Poór, M., 2020. Testing the pharmacokinetic interactions of 24 colonic flavonoid metabolites with human serum albumin and cytochrome P450 enzymes. Biomolecules 10 (3), 409.

Odle, T.G., 2014. Adverse effects of breast cancer treatment. Radiol. Technol. 85 (3), 297M–319M.

Panchal, S., Sehrawat, H., Sharma, N., Chandra, R., 2023. Biochemical interaction of human hemoglobin with ionic liquids of noscapinoids: Spectroscopic and computational approach. Int. J. Biol. Macromol. 124227.

Paolillo, M., Schinelli, S., 2019. Extracellular matrix alterations in metastatic processes. Int. J. Mol. Sci. 20 (19), 4947.

Radisky, E.S., Radisky, D.C., 2010. Matrix metalloproteinase-induced epithelial-mesenchymal transition in breast cancer. J. Mammary Gland Biol. Neoplasia 15, 201–212.

Ross, P.D., Subramanian, S., 1981. Thermodynamics of protein association reactions: forces contributing to stability. Biochemistry 20 (11), 3096–3102.

Rudra, S., Dasmandal, S., Patra, C., Mahapatra, A., 2018. Spectroscopic exploration and molecular docking analysis on interaction of synthesized Schiff base ligand with serum albumins. J. Mol. Struct. 1167, 107–117.

Safo, M.K., Abraham, D.J., 2003. X-ray crystallography of hemoglobins. Hemoglobin Disorders: Molecular Methods and Protocols, 1–19.

Salam, S., Arif, A., Nabi, F., Mahmood, R., 2023. Molecular docking and biophysical studies on the interaction between thiram and human hemoglobin. J. Mol. Struct. 1272, 134188.

Sanaei, M., Kavoosi, F., 2021. Effect of valproic acid on the class i histone deacetylase 1, 2 and 3, tumor suppressor genes p21WAF1/CIP1 and p53, and intrinsic mitochondrial apoptotic pathway, Pro-(Bax, Bak, and Bim) and anti-(Bcl-2, Bcl-xL, and Mcl-1) apoptotic genes expression, cell viability, and apoptosis induction in hepatocellular carcinoma hepg2 cell line. Asian Pac. J. Cancer Prev. 22 (S1), 89–95.

Sett, R., Paul, B.K., Guchhait, N., 2022. Deciphering the fluorescence quenching mechanism of a flavonoid drug following interaction with human hemoglobin. J. Phys. Org. Chem. 35 (3), e4307.

Shakeri, A., Delavari, S., Ebrahimi, S.N., Asili, J., Emami, S.A., Tayarani-Najaran, Z., 2019. A new tricyclic abietane diterpenoid from Salvia chloroleuca and evaluation of cytotoxic and apoptotic activities. Rev. Bras 29, 30–35.

Shen, X.-C., Liou, X.-Y., Ye, L.-P., Liang, H., Wang, Z.-Y., 2007. Spectroscopic studies on the interaction between human hemoglobin and CdS quantum dots. J. Colloid Interface Sci. 311 (2), 400–406.

Shi, D., Li, H., Zhang, Z., He, Y., Chen, M., Sun, L., Zhao, P., 2022. Cryptotanshinone inhibits proliferation and induces apoptosis of breast cancer MCF-7 cells via GPER mediated PI3K/AKT signaling pathway. PLoS One 17 (1), e0262389.

Singh, R., Letai, A., Sarosiek, K., 2019. Regulation of apoptosis in health and disease: the balancing act of BCL-2 family proteins. Nat. Rev. Mol. Cell Biol. 20 (3), 175–193.

Waks, A.G., Winer, E.P., 2019. Breast cancer treatment: a review. JAMA 321 (3), 288–300.

Wang, Y.-Q., Zhang, H.-M., Zhang, G.-C., Zhou, Q.-H., Fei, Z.-H., Liu, Z.-T., Li, Z.-X., 2008. Fluorescence spectroscopic investigation of the interaction between benzidine and bovine hemoglobin. J. Mol. Struct. 886 (1–3), 77–84.

Wang, Y.-Q., Zhang, H.-M., Zhou, Q.-H., 2009. Studies on the interaction of caffeine with bovine hemoglobin. Eur. J. Med. Chem. 44 (5), 2100–2105.

Wang, H., Zhang, Y., Zhang, Y., Liu, W., Wang, J., 2019. Cryptotanshinone inhibits lung cancer invasion via microRNA-133a/matrix metalloproteinase 14 regulation. Oncol. Lett. 18 (3), 2554–2559.

Wu, Y.-H., Wu, Y.-R., Li, B., Yan, Z.-Y., 2020. Cryptotanshinone: A review of its pharmacology activities and molecular mechanisms. Fitoterapia 145, 104633.

Yamasaki, K., Chuang, V.T.G., Maruyama, T., Otagiri, M., 2013. Albumin–drug interaction and its clinical implication. Biochimica et Biophysica Acta (BBA)-General Subjects 1830 (12), 5435–5443.

Yang, Z., Cheng, X., Li, X., 2018. Investigation of the interaction between human hemoglobin and five antioxidants by fluorescence spectroscopy and molecular modeling. J. Iran. Chem. Soc. 15, 245–257.

Ye, T., Zhu, S., Zhu, Y., Feng, Q., He, B., Xiong, Y., Zhao, L., Zhang, Y., Yu, L., Yang, L., 2016. Cryptotanshinone induces melanoma cancer cells apoptosis via ROS-mitochondrial apoptotic pathway and impairs cell migration and invasion. Biomed. Pharmacother. 82, 319–326.

Youn, H.J., Han, W., 2020. A review of the epidemiology of breast cancer in Asia: Focus on risk factors. Asian Pac. J. Cancer Prev. 21 (4), 867.

Yuan, Z., Li, Y., Zhang, S., Wang, X., Dou, H., Yu, X., Zhang, Z., Yang, S., Xiao, M., 2023. Extracellular matrix remodeling in tumor progression and immune escape: from mechanisms to treatments. Mol. Cancer 22 (1), 48.

Zeinabad, H.A., Kachooei, E., Saboury, A.A., Kostova, I., Attar, F., Vaezzadeh, M., Falahati, M., 2016. Thermodynamic and conformational changes of protein toward interaction with nanoparticles: a spectroscopic overview. RSC Adv. 6 (107), 105903–105919.

Zhang, W., Cho, W.C., Bloukh, S.H., Edis, Z., Du, W., He, Y., Hu, H. Y., Ten Hagen, T.L.M., Falahati, M., 2022. An overview on the exploring the interaction of inorganic nanoparticles with microtubules for the advancement of cancer therapeutics. Int. J. Biol. Macromol.

Zhang, Q., Wang, L., Gan, C., Yu, Y., Li, Y., Deng, Y., Liu, H., You, J., Yin, W., 2020. Cryptotanshinone induces apoptosis and inhibits migration and invasion in human hepatocellular carcinoma cells in vitro. Nat. Prod. Commun. 15, (1) 1934578X19899570.